

## Slope Shape Effects on Erosion: A Laboratory Study

D. H. Rieke-Zapp and M. A. Nearing\*

### ABSTRACT

Data on soil erosion at the slope scale is essentially limited to experiments on uniform slopes. The objective of this research was to measure the rates and patterns of erosion on complex shaped slope elements under controlled laboratory conditions where surface morphology changes could be carefully quantified. Artificial rainfall was applied for 90 min to a silt loam soil in a 4 by 4 m box. Five slope shapes were formed: uniform, concave-linear, convex-linear, nose slope, and head slope. Digital elevations models (DEMs) of the surface were measured using photogrammetry after 0, 10, 20, 40, 60, and 90 min. Slope shape had a significant impact on rill patterns, sediment yield, and runoff production. The uniform, nose, and convex-linear slopes yielded more sediment than the concave-linear and head slopes, where sediment deposited on toeslopes. Soil topography led to flow convergence and divergence, resulting in a nonuniform distribution of rill spacing and efficiency. The degree of rill incision was related to slope steepness and length, and rill success was related to the contribution area of the rill. Drainage density approached a similar value for all networks during the experiments. Development of the drainage system was similar to the development of optimum channel networks, in that during the evolution of the rill network energy expenditure was reduced. This indicated that energy expenditure was a quantifiable measure of network development and self-organization.

RECENT EXAMINATIONS of watershed-scale erosion models have revealed that while erosion models have the capability, when appropriately used, to predict runoff and sediment delivery to watershed outlets reasonably well, they are not generally effective at delineating sediment source areas within watersheds (De Roo and Jetten, 1999; Jetten et al., 1999; Kirkby and McMahon, 1999; Takken et al., 1999). One of the general conclusions that was suggested by the authors of these studies was that future modeling approaches will require more spatially detailed information on conditions such as surface topography within the watersheds. Physically based soil erosion models like WEPP (Flanagan and Nearing, 1995) or EUROSEM (Morgan et al., 1998) apply simulations on abstract topographic units that represent hillslopes or watersheds in a rather generalized way.

Advances in computer processing speeds and software algorithms allow the implementation of soil erosion models within, or linked to, geographic information systems (GIS) (e.g., Desmet and Govers, 1996; Cochrane and Flanagan, 1999). The GIS approach has the capability to reduce the level of model abstraction of watershed geometry, since topographic information in

the form of DEMs is more explicit and detailed than information often used in the past. However, to fully take advantage of information provided by the DEMs, we must have the capability to model the processes associated with erosion on complex shaped slopes, which means that we must understand the erosion processes as they occur on such slope shapes.

Favis-Mortlock (1997) identified additional shortcomings of current erosion models that are not solely related to, but certainly affected by slope uniformity and flow distribution on eroding surfaces. Watershed erosion models such as WEPP and EUROSEM are based on many a priori assumptions that do not represent microtopographic changes of an eroding surface with time. Separation of rill from interrill erosion in current erosion models makes it necessary to partition an uneroded surface, even a freshly tilled surface where no rills have developed, into rill and interrill areas before simulation starts. In the WEPP model, all rills are assumed to be equally hydrologically efficient, have a rectangular cross-section, and have a uniform spacing of 1 m (Gilley et al., 1990). The EUROSEM requires a priori knowledge of rill density as well as width, depth, gradient, side slope, and Manning's  $n$  of rills (Favis-Mortlock et al., 2000).

Erosion estimates that are calculated utilizing these generalized parameters can only be interpreted as spatially generalized results, explaining why erosion models can be calibrated to predict sediment yield from a watershed accurately, but fail to properly identify and delineate sediment source areas. Imposing the same generalized assumptions of rill network characteristics to nonuniform, complex-shaped hillslopes would also be inaccurate. Flow divergence and convergence on non-uniform slopes result in differences in hydraulic efficiency of rills (Lewis et al., 1994). Irregular topography will also result in nonuniform spacing of rills. Favis-Mortlock et al. (2000) speculated that the rill network evolving on eroding soil surfaces acts like a self-organizing dynamic system that tends toward greater orderliness. While the idea of self-organization is plausible, model implementation is still a problem.

Yang (1974) suggested, based on an analogy to thermodynamics, that during the evolution toward its equilibrium condition, a natural stream chooses its paths of flow in such manner that the rate of potential energy expenditure per unit mass of water along this course (equivalent to unit stream power) is minimum. Yang and Song (1986) hypothesized a more general theory stating that a river may adjust its flow such that the total rate of energy (or the total stream power for the case of a fixed bed) is minimized.

D.H. Rieke-Zapp, Institute for Geological Sciences, Univ. of Bern, Baltzerstr. 1, Switzerland; M.A. Nearing, USDA-ARS Southwest Watershed Research Center, Tucson, AZ 85719. Received 13 Jan. 2005.  
\*Corresponding author (mnearing@tucson.ars.ag.gov).

Published in Soil Sci. Soc. Am. J. 69:1463–1471 (2005).  
Soil & Water Management & Conservation  
doi:10.2136/sssaj2005.0015

© Soil Science Society of America  
677 S. Segoe Rd., Madison, WI 53711 USA

**Abbreviations:** DEM, digital elevation model; EUROSEM, European Soil Erosion Model; GIS, geographical information system; OCN, optimal channel network; WEPP, Water Erosion Prediction Project.

Rodriguez-Iturbe et al. (1992) postulated three principles of optimal energy expenditure as a theory for the evolution of river drainage networks. The first was the principle of minimum energy expenditure in any link of the network, the second was the equal expenditure per unit area of channel anywhere in the network, and the third was the minimum of total energy expenditure in the network as a whole. The principles are based on the assumption that flow velocity tends to be constant throughout the network. This assumption has been supported by field investigations. The three principles can be combined into one equation that applies at bank-full conditions:

$$E = \sum_{i=1}^n P_i = k \sum_{i=1}^n Q_i^{0.5} L_i \quad [1]$$

where  $E$  and  $P$  ( $\text{kg m}^2 \text{s}^{-2}$ ) are the rates of energy expenditure for the entire network and for an individual link  $i$ , respectively. The variables  $L_i$  (m) and  $Q_i$  ( $\text{m}^3 \text{s}^{-1}$ ) denote length and flow discharge in each link, respectively, and  $k$  ( $\text{kg s}^{-1.5} \text{m}^{-0.5}$ ) is a proportionality constant. The exponent of 0.5 for  $Q$  agrees well with the experimental findings of Leopold et al. (1964). By minimization of  $E$ , Rodriguez-Iturbe et al. (1992) were able to generate computer-simulated networks with properties that were similar to actual river networks.

Ijjász-Vásquez et al. (1993) defined optimal channel networks (OCNs) as networks with minimum global energy dissipation based on Eq. [1]. They simplified Eq. [1] by substituting  $Q$  with  $A$ , the contributing area for each link, based on the proportionality of link slope ( $S$ ) and  $A^{-0.5}$ :

$$E = \sum_{i=1}^n P_i = k \sum_{i=1}^n A_i^{0.5} L_i \quad [2]$$

Ijjász-Vásquez et al. (1993) have shown that the difference in total energy dissipation in simulated and real basins using Eq. [2] was small, demonstrating that river basins can be modeled as OCNs.

Gómez et al. (2003) applied the same theory to characterize self-organization of rill networks in laboratory experiments at the hillslope scale. They prepared rainfall experiments in a 2 m by 4 m box simulating three types of surface roughness for two different slope angles. Their data provided evidence that the theory is not only valid at the scale of rivers, but also on eroding hillslopes for certain cases. In all experiments with 20% slope, energy within the rill network was reduced with experimental time. For experiments with 5% slope, the treatments with medium to great roughness did not show a minimization of energy within the network in time. The authors attributed this to the fact that the initial microrelief overshadowed the general trend of minimization of energy expenditure in the evolving rill network for lower hillslope gradients.

While a considerable amount of research has been done on the effects of length and degree of slope on soil loss and runoff, only a small number of studies have focused on the effect of irregular slopes (Nearing et al., 1994). Complex slope profiles can be found in construction projects for slope stabilization and as components

of natural landscapes (Meyer and Kramer, 1969). Sediment yield from uniform slopes can be calculated from two topographic parameters, that is, average slope steepness and slope length (Smith and Wischmeier, 1957). On nonuniform slopes, local and average steepness differ considerably along the slope, consequently sediment yield from nonuniform hillslopes can vary significantly from the sediment yield experienced from uniform hillslopes (Young and Mutchler, 1969a).

Young and Mutchler (1969a, 1969b) investigated the effect of irregular slopes on soil movement and runoff. They shaped 12 field plots that were approximately 4 m wide (across slope) and 24 m long (down slope) and conducted rainfall simulation experiments on the plots. The three shape treatments included convex, concave, and linear slope shapes in downslope direction. The cross-slope component was linear for all treatments. Average slope steepness was the same for all slopes. They used fluorescent glass particles as tracers and conducted microelevation measurements at nine locations across the plots. Their results indicated that concave slopes greatly reduced the total sediment loss in comparison to a uniform or convex slope (Young and Mutchler, 1969b).

Moore and Burch (1986) developed a physically based analytical framework for predicting the consequence of topographic effects on erosion and deposition on two-dimensional and quasi three-dimensional non-planar hillslopes. The application of their model to a nonconvergent/divergent, a 20° divergent, and a 20° convergent slope showed that convergence can have a major impact on erosion, largely through the development of rills and gullies that increase erosion compared with the nonconvergent/divergent slope. Divergence had a lower predicted erosion compared with the nonconvergent/divergent case. They tested their model results on a 7.3-ha catchment that showed no apparent signs of rill erosion. The locations of zones of severe sheet erosion and gully in the catchment were in agreement with the predictions made from the analytically derived relationship based on the modeling.

The processes of soil erosion on complex-shaped hillslopes have not been studied sufficiently to take advantage of our rapidly improving ability to produce more detailed and accurate representations of hillslope surface topography. The main objective of this laboratory study was to study the effect of slope shape and the resulting divergence and convergence of flow on soil erosion, and in particular on the patterns of rill networks that form on various slope shapes. A second objective was to characterize the self-organization properties of the developing rill networks in the context of energy minimization. In addition, a technique was developed applying digital photogrammetry to produce DEMs of the soil surface with adequate temporal and spatial resolution for data analysis. The production of DEMs is discussed in more detail in Rieke-Zapp and Nearing (2005).

## MATERIALS AND METHODS

Soil surfaces were prepared in a wooden box with dimensions of 4 m × 4 m × 0.8 m, length, width, and height, respec-

tively. The bottom part of the box was filled with silica sand to allow free drainage under the soil. Depth of the sand bed ranged from 20 cm to several tens of centimeters, depending on the location in the soil box. The soil was taken from the top 0.4 m of a loess-derived, Typic Hapludalf silt-loam common in the area of West Lafayette, IN, USA. The material had a primary particle-size composition of 5% sand, 72% silt, and 23% clay, and an organic matter content of 2%. The soil was passed through an 8-mm sieve to remove the very coarse aggregates, and was loosely packed in the box on top of the sand bed.

Five slope shape treatments were used, based on the classification outlined by Ruhe (1975). The shapes were formed at different times for different experimental runs in the box (Fig. 1). A straight edge was moved across the flume on aluminum guides to shape the soil. Each slope shape used a different combination of guides and straight edges, and the position of the guides was recorded to allow replication of experiments with the same shape of the soil surface. Each slope shape experiment was replicated, for a total of 10 experimental runs. Soil depth in the flume varied between 0.15 and 0.40 m depending on how the soil was shaped and on the slope steepness. Slope shapes can be characterized by their horizontal (cross-slope) and longitudinal (down slope) curvature, as linear-linear, convex-linear, concave-linear, linear-convex, and linear-concave (Fig. 1). The flume end was straight and level by design. Consequently, cross-slope curvature of the slope was forced to become linear at the plot end and was at a maximum at the top of the flume. The effect of this arrangement was that the linear-convex slope was the shape of a nose slope and the linear-concave was the shape of a head slope. In the following text we will refer to the slope shapes as uniform, convex-linear, concave-linear, nose, and head slope as the five different slope types (Fig. 1).

Information about slope shapes was summarized in Table 1. For a better discrimination of slope shapes, maximum feasible curvature (minimum radius of curvature) was sought for in soil preparation. The radius of curvature ( $r$ ) was calculated according to Arbeitsgruppe Boden (1994) as:

$$r = \frac{e^2}{8h} + \frac{h}{2} \quad [3]$$

with geometric properties  $e$  and  $h$  as shown in Fig. 2. Average slopes were defined as average slope of the down slope profile along the center of the box. While slopes with a linear cross-slope component had very similar average slope, values for the experiments with nonlinear cross-slopes (nose and head slopes) necessarily differed due to the limitations imposed by the level outlet of the flume. Average slope in the center of the flume was a maximum for the nose slope and a minimum for the head slope (Table 1).

After every experimental run, the soil in the box was dried and raked to loosen the soil surface, break soil clods, and

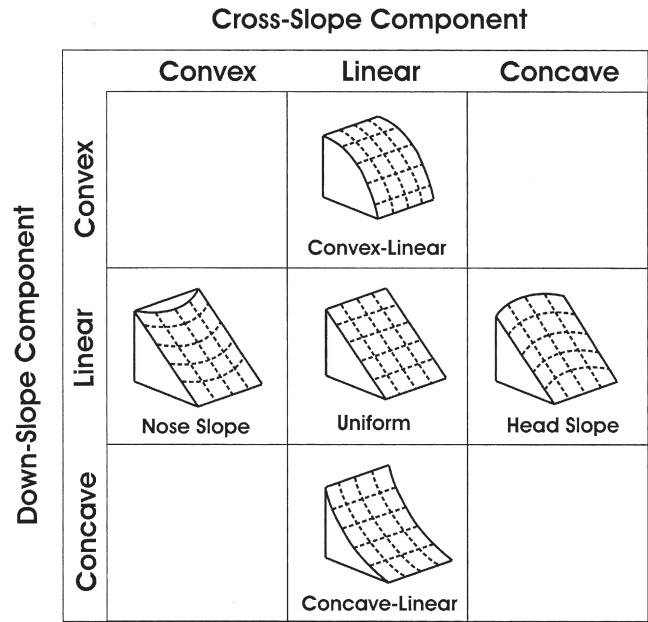


Fig. 1. Cross-slope and down-slope components of the flume experiments including naming convention. At the flume outlet all shapes were linear due to the design of the experimental box. Only components with at least one linear component could be used.

destroy surface crusts. Lost soil was replaced with fresh material to a level above that necessary, and the surface was re-shaped using the guides and straight edges as described above.

Four rainfall simulator troughs, each with four V-Jet nozzles (part No. 80100, Spraying System Co., Wheaton, IL), were raised approximately 3.70 m above the soil surface. The soil surface was prewetted multiple times with low intensity rainfall that produced only minimal amounts of runoff over a period of 5 d before the experiment. During the experiments a rainfall intensity of 60 mm h<sup>-1</sup> was applied for a total of 90 min. Rain gauges were distributed around the flume to ensure that rainfall intensity was the same in all experiments. Rainfall was stopped after 10, 20, 40, 60, and 90 min to take stereo photographs for DEM generation. Experiments lasted about 4 h from the beginning of the rainfall until the last image for DEM production was taken after the experiments. Sediment and runoff samples were collected at the flume outlet every minute for the first 40 min and then every other minute for the rest of the experiment. The flume had two troughs at the outlet, wherefore two samples were taken simultaneously and averaged for each time interval. Samples were weighed and dried at 105°C to determine the amount of sediment and runoff for each sample.

Experiments were stopped for about 20 min to wait for the soil surface to dry and to acquire images for the generation

Table 1. Characterization of slope shapes including maximum rill depth and deposition values for difference Digital Elevation Models (DEMs).

Slope shape	Radius of curvature†‡	Surface slope†§	Surface area†	Maximum erosion	Maximum deposition	Surface settling†
	m	%	m <sup>2</sup>		mm	
Concave-linear	89.5	13	18.2	51	34	5.2
Head	22.1	10	18.7	59	26	5.0
Nose	11.1	16	18.7	63	20	4.2
Convex-linear	6.0	14	18.3	88	34	2.8
Uniform	n/a	12	17.9	61	15	3.5

† Average of two replicates.

‡ Calculated according to Eq. [5] in the direction of maximum convexity/concavity.

§ Measured in the flume center from DEMs in down-slope direction.

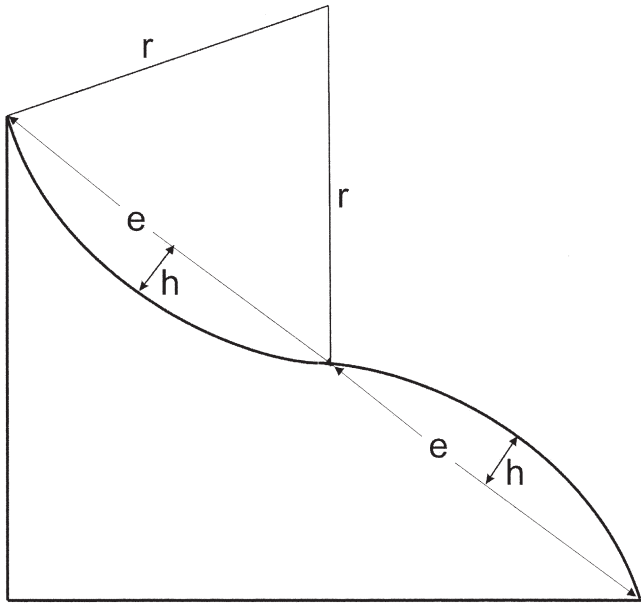


Fig. 2. Schematic for geometric properties used to calculate radius of curvature of the soil surfaces (adapted from Arbeitsgruppe Boden, 1994).

of the DEMs. A block of 16 images was needed to cover the box area with overlapping photographs that had an image scale of approximately 0.9 mm per pixel. The DEMs with a final resolution of 3-mm cell size were generated from the imagery. The DEMs of the surface were produced from images taken before the experiment and from imagery taken every time the rain was stopped. Control points were placed around the flume in such a way that they did not disturb the soil surface. A total of 60 DEMs were generated: six DEMs each for five treatments with two replicates.

The soil surface near to the plot borders was affected by plot boundary effects that changed flow direction of water, as well as soil erosion and deposition rates. To exclude these areas from the analysis, DEMs were cropped by 10 to 30 cm along the sides. All analyses were done on the cropped DEMs. The DEMs had precision of 1.2 mm in the vertical and represented the soil surface well. Details about the production of the DEMs are discussed in Rieke-Zapp and Nearing (2005).

The DEMs were used for topographic analysis of the experiments in ArcView version 3.2a (ESRI, 2000), a GIS. Rills were identified in the DEMs using SWAT software version 2.1 (Di Luzio et al., 2002), a customized plug-in for watershed analysis in ArcView GIS. For rill identification, SWAT first removed local minima (sinks) from the DEM. Flow direction on the resulting DEM was calculated by a single flow algorithm, referred to as the D8 algorithm. From the flow direction, grid flow accumulation was calculated for each grid cell. A rill was defined to begin at a point where flow accumulation of contributing cells was above a user-defined threshold. This threshold was the minimum contributing surface area of the DEM. The optimum value for the minimum contributing surface area was estimated by visual comparison of the calculated rill network with the real drainage pattern in the flume, that is, photographs and hillshading models. The minimum contributing surface area was determined for the last DEM of every experiment and the same minimum contributing surface area was applied to establish the rill network for each DEM of one experiment.

Phillips and Schumm (1987) have shown that rill spacing and drainage patterns, including the minimum contributing

surface area, change with slope steepness. This made it difficult to pick a single minimum contributing surface area threshold for an irregularly sloping surface. The variation in optimum minimum contributing surface area was most often greater within a treatment than between treatments. For this reason, we decided to use the same minimum contributing surface area for all treatments. A value of 2500 cells (225 cm<sup>2</sup>) was found to optimally represent the rill patterns of the surfaces. This procedure had the additional advantage that it allowed direct comparison of results from all experiments.

Drainage density ( $D_d$ ) was calculated according to Horton (1945):

$$D_d = \frac{\sum_{i=1}^n L_i}{A} \quad [4]$$

where  $L$  was the length of individual flow links in the drainage network and  $A$  was the area drained by the rill network. Drainage area, and flow link length for each link was determined from the SWAT output. Energy expenditure was calculated with these parameters according to Eq. [2].

## RESULTS AND DISCUSSION

### Runoff and Sediment Results

The uniform slope shape produced significantly greater ( $\alpha = 0.05$ ) runoff per unit area than the concave-linear, head, and convex-linear slopes (Table 2). The difference in runoff for the uniform slope may be partly explained by the fact that the uniform slope had the least soil surface area, which would have resulted in a reduction of surface water storage and infiltration capacity and thus increased runoff production.

Differences in sediment yield between treatments were more pronounced than for runoff (Table 2). In accord with previous literature (Young and Mutchler, 1969a, 1969b), the concave-linear treatment produced the least amount of sediment. Sediment accumulated at the bottom third of the slope (on the toeslope), reducing the measured sediment yield at the box outlet. The head slope (linear-concave) also produced significantly less sediment yield than the other three remaining treatments. The concave-linear slope had the greatest radius of curvature, while the head slope had the second greatest. In the top part of the head slope, flow was concentrated and directed toward the center leading to rill incision. Further down the slope increasingly less runoff was concentrated toward the center of the flume because the slope became linear toward the level flume outlet reducing erosion and rill incision. Rill incision (Fig. 3) decreased toward the toeslope until it stopped and sediment deposited near the flume outlets in the center of the flume. Thus, sediment yields of both slope shapes with a concave slope component were significantly less than for the other slope shapes, because sediment deposited in the toeslope region of the box. In the case of the concave-linear slope, sedimentation occurred across the entire flume width, which resulted in significantly less sediment yield than the head slope, where deposition occurred mostly in the central part of the toeslope (Fig. 3).

The uniform, nose, and convex-linear slope treat-

**Table 2. Total runoff and sediment yield by slope shape.**

Slope shape	Mean total runoff	Mean total sediment yield
	liter	kg
Concave-linear	1031 <sup>†</sup>	14.9 <sup>a</sup>
Head	1022 <sup>a</sup>	36.4 <sup>b</sup>
Nose	1091 <sup>ab</sup>	49.1 <sup>c</sup>
Convex-linear	1026 <sup>a</sup>	51.3 <sup>c</sup>
Uniform	1110 <sup>b</sup>	58.5 <sup>c</sup>

<sup>†</sup> Tukey Test groupings: means in a column followed by the same letter are not significantly different ( $\alpha = 0.05$ ).

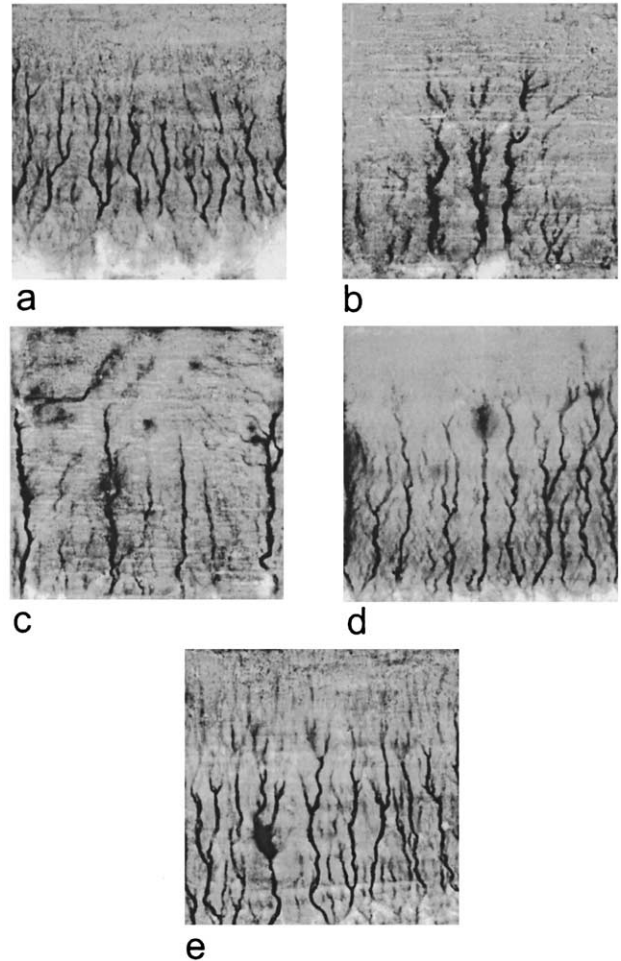
ments showed no significant difference in total sediment yield (Table 2). In the field study of Young and Mutchler (1969a, 1969b), the convex-linear slope produced the largest sediment yield and the concave-linear produced the least. In the study presented here, the concave-linear slope also produced the lowest sediment yield.

Figure 3 also revealed that sediment was accumulated in the toe slope region of the convex-linear slope immediately adjacent to the flume boundary, thus reducing sediment collected at the flume outlet. This was probably due to plot end effects. Rill incision started half-way down the convex-linear slope and rills cut deeper than for any other treatment (up to 88 mm, Table 2). The box outlet marked the physical erosion base level of the flume, which was fixed. This limited rill incision toward the flume outlet. Rill incision of the convex-linear slope was significantly reduced approximately 20 cm before the flume outlet. The local erosion base level was reached and sediment started to accumulate across the width of the flume. The uniform slope was less affected by the plot end effect and more soil material was able to pass the flume boundary and be collected at the flume outlet. Another reason that could explain the differences to Young and Mutchler's (1969a, 1969b) findings (i.e., that the convex-linear slope produced more sediment than the uniform slope) was that slope length in their experiments was 24 m compared with only 4 m in the flume study presented here. As a result, the largest degree of curvature for the convex-linear (VL) slope in this experiment was located approximately two-thirds downslope and thus only 1.3 m above the flume outlet. This distance may not have been long enough to reproduce the findings of the field study by Young and Mutchler (1969a, 1969b).

The difference DEMs (indicating the elevational differences between sequential DEMs) presented in Fig. 3 can be used to illustrate surface evolution, but could not be used for quantification of soil loss. Soil loss calculated from comparing the surface before and after the experiment was considerably greater than the amount of sediment collected at the flume outlet. This was attributable to settling of the soil during the experiment. Comparing the amount of sediment yield collected at the flume outlet with soil loss on the flume calculated from difference DEMs resulted in a settling amount of the soil of up to 5.2 mm (Table 1). The settling amount was calculated from the following relationship:

$$S_y = D_B \times n \times 0.09 \text{ cdZ} \quad [5]$$

where  $S_y$  was sediment yield,  $D_B$  bulk density (1.35 g



**Erosion** **Deposition**

**Fig. 3. Difference digital elevation models (DEMs) for the simulated slope shapes calculated from DEMs showing the difference in topography before and after 90 min of rainfall for: (a) concave-linear, (b) head slope, (c) nose slope, (d) convex-linear, and (e) uniform treatments. DEMs were adjusted for settling of soil according to Table 1. The area of each difference DEM is approximately 3.8 m by 3.8 m. All DEMs are oriented in such way that the top of the flume is directed to the top of the page and the bottom of the flume is toward the bottom of the page. Relative erosion and deposition of sediment can be estimated from the gray-scale bar. Absolute numbers of maximum erosion and deposition for each treatment are reported in Table 2.**

$\text{cm}^{-3}$ ) of the prepared soil,  $n$  was the number of pixels in the difference DEMs (each having an area of  $0.09 \text{ cm}^2$ ),  $c$  was a proportionality constant relating the area of the analyzed DEM to the area of the total flume, and  $dZ$  was the mean elevation difference of the DEMs.

The degree of erosion and rill incision was related to slope steepness and length as well as upslope conditions of the surface. All treatments with a linear cross-slope component developed a drainage network with parallel rills. This was in accord with the findings of Phillips and Schumm (1987). Continuous rills carved deeper with increasing slope length in the uniform slope treatment. Rilling in the convex-linear treatment began further downslope since slope steepness of the upslope compo-

ment was less than for the uniform slope treatment. Slope in the concave-linear slope treatment was steepest at the upper part and gradually declined from the flume center toward the outlet, thus relatively deep rill incision occurred the upper part of the slope. The maximum rill depth was found at the center of the flume.

Rill incision was more complex for the head and nose slope treatments, the two treatments with a nonuniform cross-slope slope component. In general, rill incision followed the steepest slope and caused divergence of flow lines in the case of the nose slope and convergence in case of the head slope. In the case of the head slope, flow lines converged toward the center of the flume and water cut deep into the soil matrix. In the nose slope treatment, flow was directed toward the edges of the flume and concentrated flow started to incise deep rills in these areas. Since slope shape tapered off toward the outlet, rill orientation was redirected and became parallel toward the box outlet. While rill spacing became more uniform in this area, observed discharge and size of the rills reflected the upslope conditions. While the drainage system became more parallel, width and depth of rills indicated rill 'success' that depended on the upslope contributing area of rills.

These findings illustrated that slope shape had a significant impact on soil loss and rill incision patterns (Fig. 4). Flow concentration was the main factor for rill incision. It was controlled by slope direction as well as upslope conditions, that is, slope steepness and contributing area. This confirms that the assumption of uniformly spaced and equally efficient rills that is used in many process-based soil erosion models is problematic, as has been suggested previously by Favis-Mortlock et al. (2000). Our study shows that the assumption is particularly inappropriate for non-uniform slope shapes, which are the norm for natural slopes. Testing this data set against the RILLGROW model by Favis-Mortlock et al. (2000) could reveal if this model is capable of predicting emergent surface features that are controlled by slope shape at the laboratory plot scale.

In terms of implications of these results for landscape evolution, it is worthwhile to understand that the erosion pattern is not controlled by the sediment yield. Usually the head slope is a region of backcutting into the landscape, so it is generally an active eroding area relative to the nose slope, which is a divergent flow area. Our experiments showed greater sediment yield from the nose slope treatment, but this was because of two reasons: (i) there was deposition of eroded material at the base of the head slope, and (ii) much of the erosion from the nose slope actually occurred along the side boundaries of the bed (Fig. 3c and 4c), which would actually be a concentrated flow area within the context of the landscape. In fact, significant rilling did occur in the central region of the head slope, which would result in backcutting within the context of a landscape.

### Temporal Evolution of Erosion Patterns and Self-organization

Six DEMs were generated for each experiment to study the temporal development of the rill network with

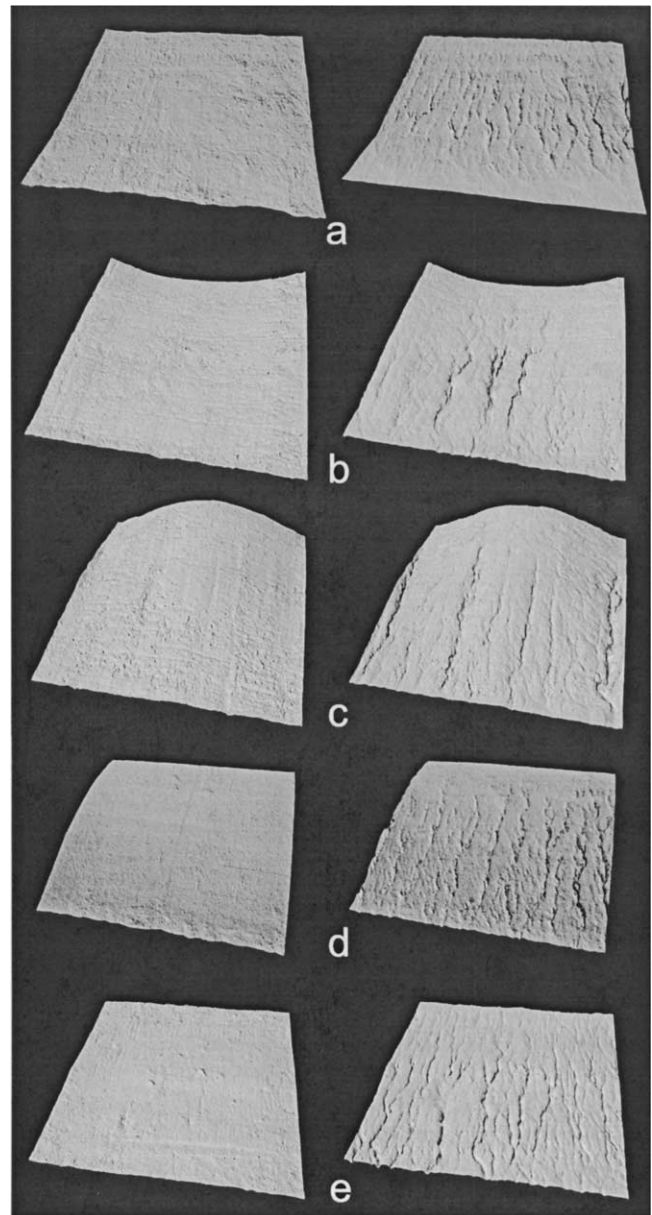


Fig. 4. Digital elevation models (DEMs) showing surface morphology before and after 90 min of rainfall for: (a) concave-linear, (b) head-slope, (c) nose-slope, (d) convex-linear, and (e) uniform treatments. The area of each difference DEM is approximately 3.8 m by 3.8 m.

time. Network composition can be studied from vector files that were generated from flow accumulation grids using the SWAT software package. Since the network data lack information about width or depth of flow links, the three-dimensional development of the network was best studied in hillshading models. An example for rill development is shown in Fig. 5.

Govers and Poesen (1988) have shown that the relative importance of rill and interrill erosion contributions change during the development of the drainage network on a soil surface. During the first stage of surface development interrill erosion is dominant. Throughout the expansion of the rill network in the second stage of development, rill erosion is the major component of erosion. After the rill network is fully developed and

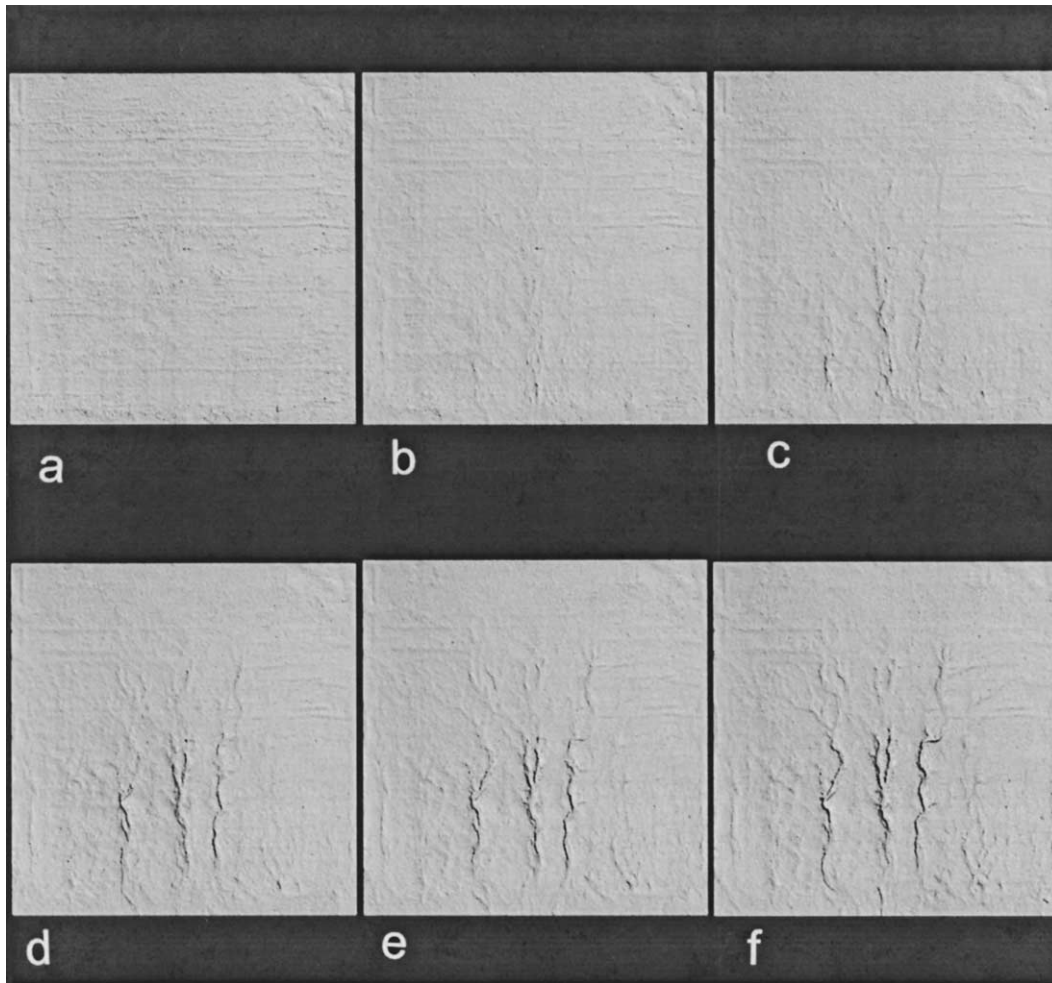


Fig. 5. Time sequence of surfaces for one of the linear-concave experimental runs: (a)  $t = 0$ , (b)  $t = 10$  min, (c)  $t = 20$  min, (d)  $t = 40$  min, (e)  $t = 60$  min, (f)  $t = 90$  min.

the surface tends toward equilibrium, interrill erosion may become the most dominant erosion process again. Such development can be inferred from Fig. 5. During the first 10-min rill incision was minor, and from  $t = 20$  min until  $t = 90$  min the rill network developed. It was not clear if the drainage network reached the stage of quasi-equilibrium after 90 min of the experiment, although Fig. 5 suggested that the whole surface area was well-drained after 90 min and we can assume that only minor adjustment would probably taken place if rain were continued.

Drainage density of all networks increased with time (Fig. 6). This indicated that total stream length was increasing since drainage area was practically constant with time. A greater drainage density relates to a better-drained surface (Horton, 1945). Phillips and Schumm (1987) have shown that drainage density increases with increasing slope steepness. In this study drainage density was similar in all treatments after 90 min. The influence of the complex topography with varying local slope steepness appeared to have only little influence on drainage density.

Local slope steepness was reflected in the incision rate and depth of rills, but was not reflected in drainage

density. Further experiments with varying soil types could show if this is a universal behavior. Drainage density was calculated from the two-dimensional area of the plot and the one-dimensional stream length. Flow width or depth was not included in the calculation of drainage density. These two parameters are closely related to rill discharge and rill success. Therefore, it may be difficult to relate rill success or the self-organization of the rill network to drainage density.

A self-organizing system will organize in such way that local entropy decreases with time (Favis-Mortlock et al., 2000). This idea is similar to the theory of the minimization of energy expenditure that was proposed Ijjász-Vázquez et al. (1993). Energy expenditure was calculated using Eq. [2]. Energy expenditure ultimately became less as a function of time in the networks of all the slope shapes (Fig. 7), though the response of the head slope was somewhat delayed. It is not entirely clear why this delay occurred for the head slope treatment. The theory of energy expenditure is based on the assumption that flow velocities of all network links were similar within the network. This appears to be a reasonable assumption for these experiments, particularly since Govers (1992) and Nearing et al. (1997) have shown that flow

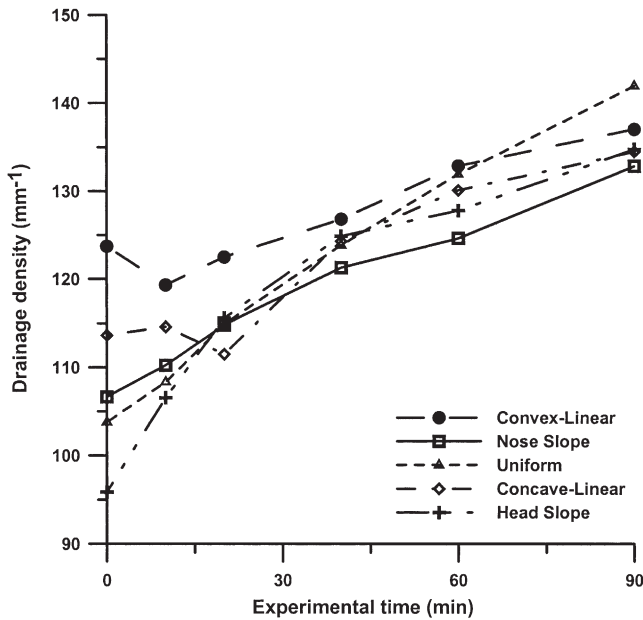


Fig. 6. Drainage density of the rill networks that developed on the soil surface as a function of rainfall simulation time.

velocities in eroding rills do not vary significantly with slope. However, for the head slope treatment this assumption may have been violated because of the very large change in slope at the end of the soil bed. Still, if this is the reason for the difference on this treatment, it is not clear why the same phenomenon would not have occurred for the concave-linear slope, also.

In summary, the energy expenditure in this experiment appeared to be a physical measure for self-organization of the drainage networks, which would indicate that the basic theory may hold for many cases at this scale as well as the larger, river scale. These findings are similar to the ones found by Gómez et al. (2003) using a 4 m by 2 m soil bed.

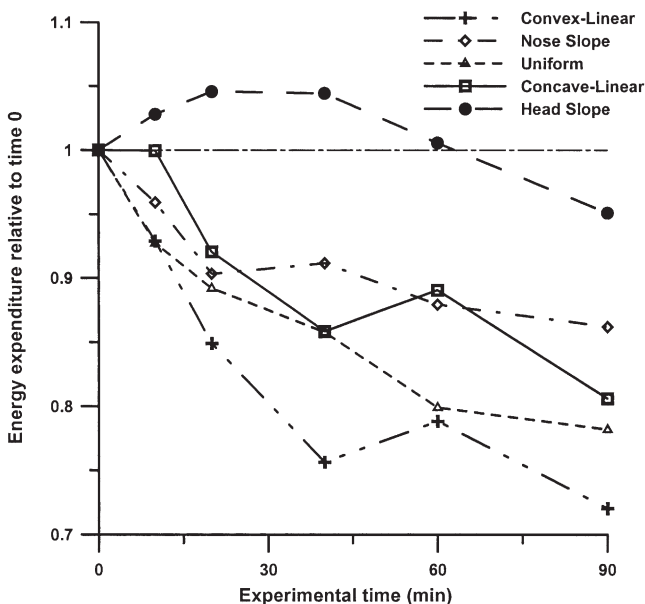


Fig. 7. Normalized energy expenditure of the rill networks, calculated using Eq. [2], as a function of rainfall simulation time.

While it appears that river and rill drainage networks may tend toward self-organization and minimization of energy expenditure in a similar manner, the processes controlling network development in both cases are somewhat different. While microtopography, rain splash, soil aggregation, and surface crusting play an important role in the development of a drainage network evolution under simulated rainfall conditions in small plots (i.e., Gómez, 2003; Favis-Mortlock et al., 2000; Hancock and Willgoose, 2001), other parameters like precipitation, macrotopography and the underlying geologic structures play an important role in river network evolution (Zernitz, 1932; Horton, 1945). Abrahams (1984) also emphasized that most humid region river networks are fed by groundwater, while hillslope drainage systems are often controlled by surface runoff evoked from rainfall. Thus, the evolution of drainage networks are controlled by different factors at different scales. It is thus interesting that ultimately the reduction of energy expenditure appeared to be a quantifiable behavior of these drainage networks as they have been shown to be for river scale networks.

## CONCLUSIONS

Quick data acquisition times and a large vertical range of DEMs derived from stereo photographs allowed the in-depth study of eroding soil surfaces with different slope shapes. DEMs were employed to identify the spatial and temporal distribution of erosion patterns on the surface. After adjusting for the settlement of the soil, the DEMs could be used to identify sediment source areas and the emergent drainage network.

Slope shape had a significant impact on rill patterns, sediment yield, and runoff production. The uniform, nose, and convex-linear slopes yielded more sediment than the concave-linear and head slopes. In general, for cases where sediment deposited on toeslopes, the sediment yields were lower. Soil topography led to flow convergence and divergence, resulting in a nonuniform distribution of rill spacing and efficiency. Distribution of rills was related to slope steepness, and rill success was related to the contributing area of the rill.

Drainage density approached a similar value for all networks during the experiments. This indicated that slope shape appeared not to have influenced the drainage density. Development of the drainage system, however, was similar to the development of optimum channel networks, in that during the evolution of the rill network, energy expenditure was reduced. This indicated that energy expenditure of the network could be used as a quantifiable measure of network development and self-organization. It would be useful to further investigate this phenomenon, perhaps through the application of an evolutionary rill generation model such as RillGrow (Favis-Mortlock et al., 2000), for instance.

Future erosion prediction models should incorporate the dynamic changes of the soil surface with time. The a priori assumptions that current soil erosion prediction models use, such as WEPP and EUROSEM are based on, cannot simulate the emergence of a rill network, es-

pecially on non-uniform shaped slopes. Applying erosion prediction models in a realistic spatial and temporal domain should increase the accuracy of soil erosion prediction models. Application of photogrammetry at the plot to watershed scale could provide topographic data with more adequate spatial resolution than publicly available data sets. Such data could be used to study on-site processes within a watershed and to validate a future generation of erosion prediction models.

## REFERENCES

- Abrahams, A.D. 1984. Channel networks: A geomorphological perspective. *Water Resour. Res.* 20:161–168.
- Arbeitsgruppe Boden. 1994. *Bodenkundliche Kartieranleitung*. 4th ed. Hannover, Germany.
- Cochrane, T.A., and D.C. Flanagan. 1999. Assessing water erosion in small watersheds using WEPP with GIS and digital elevation models. *J. Soil Water Conserv.* 54:678–685.
- Di Luzio, M., R. Srinivasan, J.G. Arnold, and S.L. Neitsch. 2002. Soil and water assessment tool. ArcView Gis Interface Manual: Version 2000. GSWRL Report 02-03, BRC Report 02-07, published by Texas Water Resources Institute TR-193, College Station, TX.
- De Roo, A.P.J., and V.G. Jetten. 1999. Calibrating and validating the LISEM model for two data sets from the Netherlands and South Africa. *Catena* 37:477–493.
- Desmet, P.J.J., and G. Govers. 1996. A GIS procedure for automatically calculating the USLE-LS factor on topographically complex landscape units. *J. Soil Water Conserv.* 51:427–433.
- ESRI. 2000. ArcView. 3.2a users manual. Environmental Systems Research, Redlands, CA.
- Favis-Mortlock, D.T. 1997. A self-organizing dynamic systems approach to the simulation of rill initiation and development on hillslopes. *Comput. Geosci.* 24:353–372.
- Favis-Mortlock, D.T., J. Boardman, A.J. Parsons, and B. Lascelles. 2000. Emergence and erosion: A model for rill initiation and development. *Hydrol. Process.* 14:2173–2205.
- Flanagan, D.C., and M.A. Nearing. 1995. USDA-Water Erosion Prediction project: Hillslope profile and watershed model documentation. NSERL Report No. 10. USDA-ARS National Soil Erosion Research Laboratory, West Lafayette, IN.
- Gilley, J.E., E.R. Kottwitz, and J.R. Simanton. 1990. Hydraulic characteristics of rills. *Trans. ASAE* 33:1900–1906.
- Gómez, J.A., F. Darboux, and M.A. Nearing. 2003. Development and evolution of rill networks under simulated rainfall. *Water Resour. Res.* 39:1148.
- Govers, G. 1992. Relationship between discharge, velocity, and flow area for rills eroding loose, non-layered materials. *Earth Surf. Processes Landforms* 17:515–528.
- Govers, G., and J. Poesen. 1988. Assessment of the inter-rill and rill contributions to total soil loss from an upland field plot. *Geomorphology* 1:343–354.
- Hancock, G., and G. Willgoose. 2001. The interaction between hydrology and geomorphology in a landscape simulator experiment. *Hydrol. Process.* 15:115–133.
- Horton, R.E. 1945. Erosional development of streams and their drainage basins: Hydrophysical approach to quantitative morphology. *Bull. Geophys. Soc. Am.* 56:275–370.
- Ijjász-Vásquez, E.J., R.L. Bras, I. Rodriguez-Iturbe, R. Rigon, and A. Rinaldo. 1993. Are river basins optimal channel networks? *Adv. Water Res* 16:69–79.
- Jetten, V., A.P.J. De Roo, and D.T. Favis-Mortlock. 1999. Evaluation of field-scale and catchment-scale soil erosion models. *Catena* 37:521–541.
- Kirkby, M.J., and M.L. McMahon. 1999. MEDRUSH and the Castop basin—The lesson learned. *Catena* 37:495–506.
- Leopold, L.B., M.G. Wolman, and J.P. Miller. 1964. *Fluvial Processes in Geomorphology*. W.H. Freeman, New York.
- Lewis, S.M., B.J. Barfield, D.E. Storm, and L.E. Ormsbee. 1994. PRORIL—An erosion model using probability distributions for rill flow and density: 1. Model development. *Trans. ASAE* 37:115–123.
- Meyer, L.D., and L.A. Kramer. 1969. Relation between land-slope shape and soil erosion. *Agric. Eng.* 50:522–523.
- Moore, I.D., and G. J. Burch. 1986. Modelling erosion and deposition: Topographic Effects. *Trans. ASAE* 24:1624–1630, 1640.
- Morgan, R.P.C., J.N. Quinton, R.E. Smith, G. Govers, J.W.A. Poesen, K. Auerswald, G. Chisci, D. Torri, and M.E. Styczen. 1998. The European Soil Erosion Model (EUROSEM): A dynamic approach for predicting sediment transport from fields and small catchments. *Earth Surf. Processes Landforms* 23:527–544.
- Nearing, M., L. Lane, and V. Lopes. 1994. Modeling Soil Erosion; p. 126–156. *In* R. Lal (ed.) *Soil erosion research methods*. 2nd ed. Soil and Water Conservation Society and St. Lucie Press; Delray Beach, FL.
- Nearing, M.A., L.D. Norton, D.A. Bulgakov, G.A. Larionov, L.T. West, and K.M. Dontsova. 1997. Hydraulics and erosion in eroding rills. *Water Resour. Res.* 32:865–876.
- Phillips, L.F., and S.A. Schumm. 1987. Effects of regional slope on drainage networks. *Geology* 15:813–816.
- Rieke-Zapp, D.H., and M.A. Nearing. 2005. Digital close range photogrammetry for measurement of soil erosion. *The Photogrammetric Record*. 20:69.
- Rodriguez-Iturbe, I., A.R. Rinaldo, R. Rigon, R.L. Bras, A. Marani, and E. Ijjász-Vásquez. 1992. Energy dissipation, runoff production, and the three-dimensional structure of river basins. *Water Resour. Res.* 28:1095–1103.
- Ruhe, R.V. 1975. *Geomorphology*. Houghton Mifflin Co. Publishers, Boston.
- Smith, D.D., and W.H. Wischmeier. 1957. Factors affecting sheet and rill erosion. *Trans. Am. Geophys. Union* 38:889–896.
- Takken, I., L. Beusenlinck, J. Nachtergaele, G. Govers, J. Poesen, and G. Degraer. 1999. Spatial evaluation of a physically-based distributed erosion model (LISEM). *Catena* 37:431–477.
- Yang, C.T. 1974. On river meanders. *J. Hydrol. (Amsterdam)* 13: 231–253.
- Yang, C.T., and C.C.S. Song. 1986. Theory of minimum energy and energy dissipation rate. p. 353–399. *In* N.D. Chermisinoff (ed.) *Encyclopedia of fluid mechanics*. Gulf, Houston, TX.
- Young, R.A., and C.K. Mutchler. 1969a. Soil movement on irregular slopes. *Water Resour. Res.* 5:1084–1089.
- Young, R.A., and C.K. Mutchler. 1969b. Effect of slope shape on erosion and runoff. *Trans. ASAE* 12:231–233, 239.
- Zernitz, E. 1932. Drainage patterns and their significance. *J. Geol.* 40:498–521.